Sensors and Actuators B 181 (2013) 523–528

Contents lists available at SciVerse ScienceDirect

Sensors and Actuators B: Chemical

journal homepage: www.elsevier.com/locate/snb

Detection of ethanol and water vapor with silicon quantum dots coupled to an optical fiber

Z.H. Zhang[a,b], R. Lockwood[b], J.G.C. Veinot[c], A. Meldrum[b,*]

[a] School of Physical Electronics, University of Electronic Science and Technology of China, Chengdu 610054, PR China
[b] Department of Physics, University of Alberta, Edmonton, AB T6G2E1, Canada
[c] Department of Chemistry, University of Alberta, Edmonton, AB T6G2G2, Canada

ARTICLE INFO

Article history:
Received 23 November 2012
Received in revised form 14 January 2013
Accepted 17 January 2013
Available online 4 February 2013

Keywords:
Silicon nanocrystals
Quantum dots
Fiber optic
Sensor
Ethanol
Water
Vapor
Gas

ABSTRACT

The end facet of a standard multimode optical fiber was coated with fluorescent silicon quantum dots (Si-QDs) and used as a probe to detect water and alcohol vapors as a feasibility study for sensing applications. In this work, the response of the sensor to different analytes was observed, and the repeatability of the sensor response was investigated. When exposed to different vapors, the luminescence intensity of the Si-QDs varied over timescales of a few seconds to hours. By coupling the QDs to an optical fiber splitter, fiber-based measurements were demonstrated for ethanol and water vapor. At this stage, the Si-quantum-dot-based fiber sensing shows a fast response time and reasonable detection limits, but true quantification remains difficult owing in part to sample-to-sample variations.

1. Introduction

Optical fiber sensors present a vast array of practical remote sensing devices. They can be used to sense changes in strain [1], temperature [2], pressure [3], vibration and acceleration [4], and local electromagnetic fields [5]. They can perform refractometry [6] and measure solution properties such as pH and pO_2 [7], and they are finding a wide range of uses in biomedical analysis [8,9]. Efforts have been made toward the development of a fiber optic sensor for volatile organics [10], for the remote analysis of toxic or explosive gases [11,12] or for the detection of organic contaminants in groundwater [13]. Fiber sensors for measuring the ethanol concentration in alcoholic beverages [14] and in gasoline [15] have been reported. Optical sensors for ethanol vapors based on absorption of ethanol on ZnO particles attached to microring resonators [16,17], nanorods [18], or thinned optical fibers [19] have also been reported. Surface plasmon resonances of silver particles coupled to an optical fiber have also been used for ethanol sensing [20].

Silicon-based detectors can be advantageous because of their benign chemistry, relative ease of handling, and low toxicity in biological environments [21]. Porous silicon (PSi) has been much studied for vapor sensing applications [22–24] due to its large surface area and wide range of transduction mechanisms, but the material is fragile and difficult to interface with an optical fiber. In one case, a planar PSi microcavity structure was adhered to one end of a bifurcated fiber [25]. When exposed to either humidity or one of three different volatile hydrocarbons, the cavity resonance shifted to longer wavelengths as measured by light injected through one arm of the fiber, reflected from the cavity, and analyzed by a spectrometer.

We previously showed that when freestanding (i.e., not embedded in a matrix) Si-QDs are exposed to blue or UV light in room air, the luminescence intensity can increase by a factor of at least 10 [26]. This process is called "photoactivation". Fourier-transform infrared spectroscopy (FTIR) was used to show that photoactivation occurs in a two-step process. The first step involved the breaking of Si—H surface terminations, leaving behind a non-radiative trap (possibly the neutral P_b center). During this rapid initial stage, the fluorescence intensity decreases and the fluorescence lifetimes shorten. The second step involves the oxidation and hydration of the dangling bonds, which leads to a prolonged gradual increase in the emission intensity over a period of hours in room air [26]. During this stage, signals from hydride and oxide surface bonds were observed to grow stronger with activation time.

In most synthesis methods the Si-QDs are encapsulated in a solid matrix. While advantageous for certain applications, solid

* Corresponding author. Tel.: +1 780 492 5342.
E-mail address: ameldrum@ualberta.ca (A. Meldrum).

0925-4005/$ – see front matter © 2013 Elsevier B.V. All rights reserved.
http://dx.doi.org/10.1016/j.snb.2013.01.070

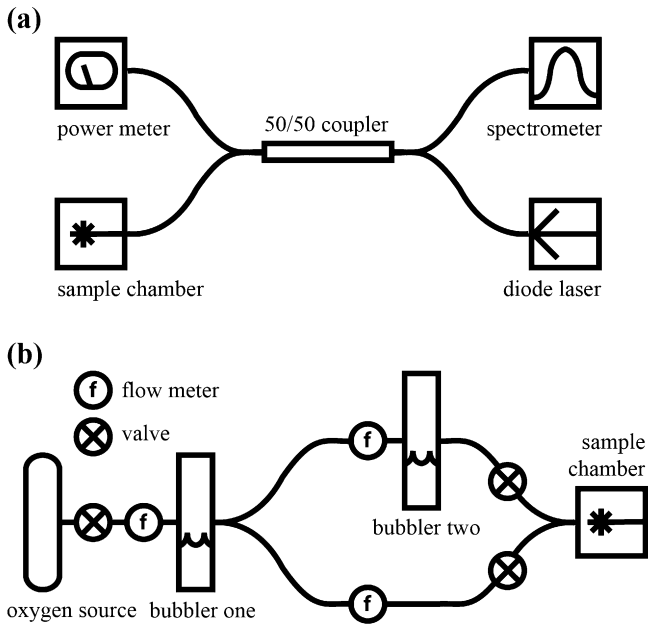

Fig. 1. (a) Diagram of the sensor structure and (b) diagram of the layout for the vapor sensing experiments.

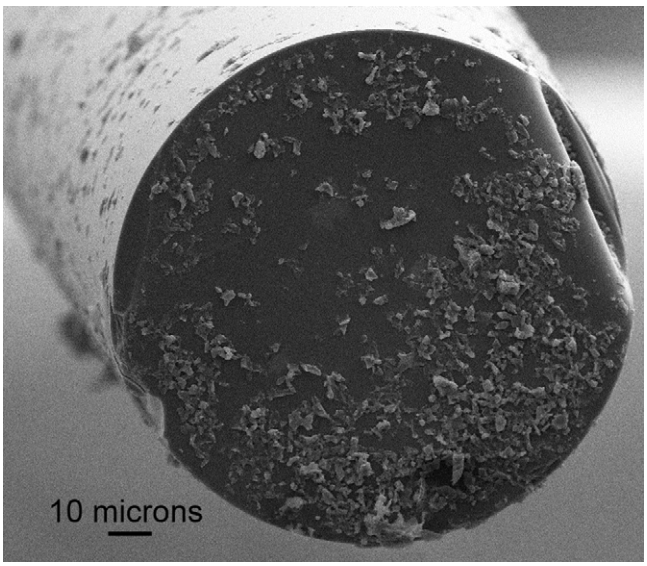

Fig. 2. Topographic SEM image showing the sensor end of a fiber. The Si-QDs appear as small clumps on the cleaved end of the fiber, and along the length of the fiber that was dipped into the solution.

encapsulation isolates the QDs from the environment and physically blocks their response to the surrounding atmosphere. The objective of the present work was, therefore, to integrate freestanding (un-encapsulated) Si-QDs into a fluorescence sensor structure. We use a basic fiber-coupled design to detect water and ethanol vapors, using the quantum-dot photoactivation property as the transduction mechanism.

2. Materials and methods

The Si-QDs were prepared in bulk by dissolution from a silica-like matrix [27]. Briefly, the procedure involved annealing gram quantities of hydrogen silsesquioxane ($H_{12}Si_8O_{12}$) for one hour at 1100 °C under an atmosphere consisting of 95% Ar + 5% H_2. This produced a tan-colored powder of consisting of Si-QDs embedded in a silica matrix. The powder was then mechanically pulverized and the Si-QDs were subsequently freed from the silica matrix by etching for 15 min in a solution of 7.5 mL HF (49%, v/v aqueous) + 0.2 mL HCl (37%, v/v aqueous). This was followed by an additional 5-min etch with 5.0 mL of ethanol (95%, v/v aqueous) added to the HF + HCl solution. The suspended QDs were then extracted into toluene. The toluene was evaporated until a relatively high concentration of particles in solution was obtained.

The sensor structure was designed using a 2×2 optical fiber coupler (Fig. 1a) with 50% coupling at 800 nm, near the peak fluorescence wavelength of the Si-QDs. Light from a blue diode laser was coupled into one arm of the fiber coupler. A layer of Si-QDs was deposited on the opposite end of the same arm of the fiber coupler, by dipping one end of the cleaved fiber into the QD solution and allowing it to dry in ambient conditions. The QD-coated end of the fiber coupler was inserted into an environmentally sealed chamber with a volume of ~30 mL. Fluorescence from the Si-QDs was collected by the same arm of the fiber and evanescently transferred to the third arm of the coupler. This was attached to an Ocean Optics USB2000 spectrometer. The fourth arm of the coupler was used to monitor the power and stability of the pump laser. The coupling efficiency ratio was found to be about 2:1 at the 445 nm laser wavelength, so the QDs were always placed on the higher-pump-power arm (~80 μW emitted from the fiber tip).

To characterize the response of the sensor to different analytes, the sample chamber was partly filled with liquid, in order to obtain a saturated vapor pressure. The analytes tested were water, a 50% (v/v) mixture of ethanol and water, and 100% anhydrous ethanol, all with room air in the chamber. Calibration tests were also done using only air or 99.998% O_2 gas in the chamber, without an analyte liquid. A blank run was also performed in each set of experiments, without the Si-QDs on the fiber tip.

In order to measure the repeatability of the sensor response, a similar gas chamber was used. A gas manifold linked two gas lines to the same input line on the chamber (Fig. 1b). One line flows through bubbler 2, which contained water, ethanol or a mixture of the two liquids. The carrier gas was 99.998% dry O_2. The other line delivered only O_2 to the chamber. In order to measure the response to water and ethanol vapor, a set of valves diverts the flow from the dry line to the bubbler line. Thus, switching from the dry O_2 line to the bubbler-2 line could be repeated as often as desired. A second bubbler (bubbler 1) could be inserted before the gas manifold, for cases (as described below) in which both vapors of water and ethanol were needed in the same run.

3. Results

The Si-QDs formed micron-scale "clumps" on the end facet of the sensor arm of the fiber coupler (Fig. 2). The luminescence from the QDs was readily detectable (Fig. 3), initially peaking at a wavelength near 750 nm. With the chamber sealed with dry O_2 the fluorescence intensity decreased relatively quickly over the first 30 min, followed by a more gradual continuous decrease. In room air (i.e., no liquid in the chamber, 40% relative humidity), the integrated photoluminescence intensity decreased initially, followed by a slow continuous increase over 60 min, consistent with previous results for QDs deposited on a wafer [26].

The sensorgrams in Fig. 4 highlight the different responses to different analytes in the chamber. The integrated intensity of first spectrum was subtracted from all the integrated intensity measurements. This effectively "subtracted out" underlying contributions from the fiber (which showed background luminescence) and the variations in QD concentration on the fiber tips. With water in the chamber, the PL intensity increased strongly over the first 10 min before approaching saturation. With ethanol in the

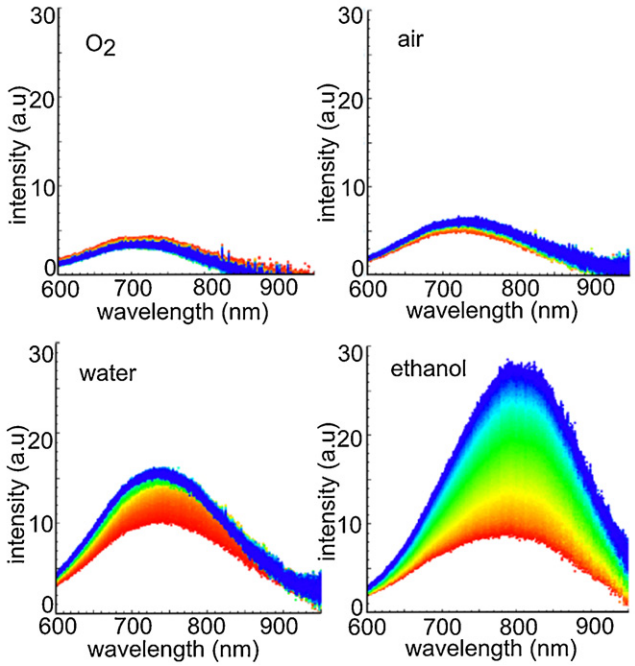

Fig. 3. Fluorescence spectra from the Si-QDs on the end of a fiber coupler, in various static atmospheres. The collection interval was 30 s. The colors red to blue represent successive spectra taken over a period of 1 h. (For interpretation of the references to color in this figure legend, the reader is referred to the web version of the article.)

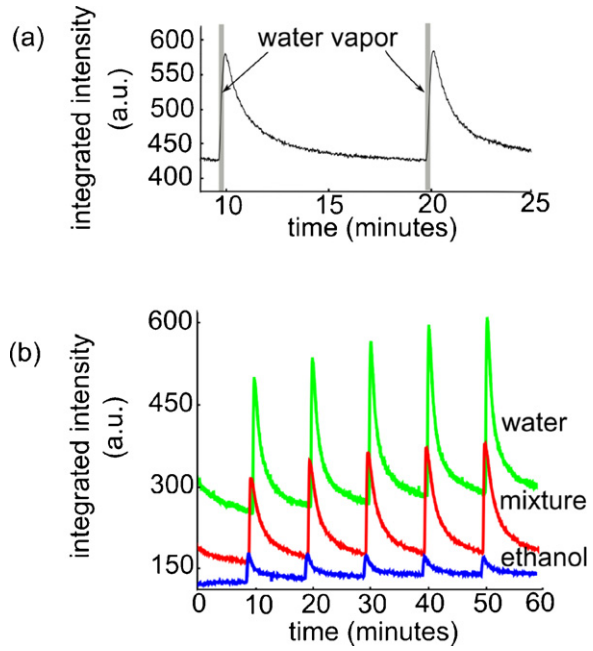

Fig. 5. Sensor response (integrated intensity) to repeated 15-s exposures to saturated water vapor, ethanol vapor, or a 50% mixture of both, using O_2 as the carrier gas. Data offset for clarity. The inset shows the timing of the 15-s vapor-injection intervals superimposed on the sensor response.

chamber, the curve was somewhat different: in this case it showed a sigmoidal shape, increasing slowly at first but then increasing more quickly. The water–ethanol mixture showed a behavior intermediate between those for the two pure liquids. With dry O_2 in the chamber, there was a gradual decrease in the integrated intensity over time. For all the curves in Fig. 4, there was no gas flow through the chamber: the chamber was simply sealed with the various samples inside.

Having established the baseline sensor response, the repeatability was measured next. From the basic activation curves in Fig. 4, alternating between either water or ethanol (showing a fluorescence intensity increase) and dry O_2 (showing a decrease) could permit the sensor response to be cycled. Thus, for these

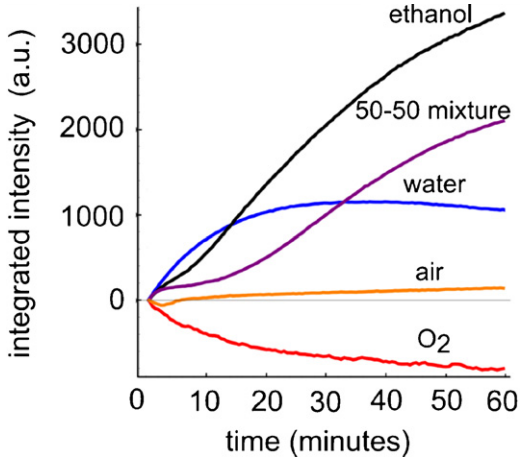

Fig. 4. Integrated fluorescence intensity as a function time for the Si-QD fiber sensor in O_2, room air, and air saturated with water, ethanol, or a 50% mixture of both. All data collected at room temperature. In order to facilitate comparisons between different samples, the first data point of each series was assumed to have a zero arbitrary intensity value. Thus, for an O_2 ambient, we see that the intensity decreased after the first measurement.

experiments, O_2 gas was flowed into the sample chamber at a rate of 0.13 L/min. The O_2 gas flow was diverted through the bubbler for periods of 15 s every 10 min. In order to compare the sensor response, experiments were conducted with water, ethanol, or a 50% by volume mixture in the bubbler.

The sensor response was found to be repeatable (Fig. 5). After a 15-s-long injection of the saturated vapor the fluorescence intensity increased sharply, reaching a maximum value approximately 16 s after the bubbler valve was opened. This is approximately equal to the calculated delay based on the measured flow rate and the bubbler-to-chamber tubing volume, implying that the sensor response is fast. The luminescence then decayed over a period of about 2 min, reaching a level close to the original value. In various experiments, the sensor was tested up to 30 consecutive times; the response was found to be repeatable, although with a slight background variation in the luminescence intensity. Furthermore, the response was different for each vapor; it was largest for water vapor, smallest for ethanol, and intermediate for mixtures of the two. This behavior is consistent with the "static" results in Fig. 3, which showed the fastest initial increase for water.

We next performed consecutive water and ethanol sensor response measurements on the same sample. One sample was first exposed to five cycles with water in the bubbler. The bubbler was then emptied, rinsed, re-filled with ethanol, and five further cycles were conducted with ethanol vapor. The same experiment was then repeated in reverse order for a second sample (ethanol first, then water). The results showed reasonable consistency; the response was always greatest for water (Fig. 6). The responses did not completely mirror each other, however. When water vapor was injected first, the sensor response to ethanol was slightly larger than it was otherwise.

The sensor response to water and ethanol (and the mixture) might be difficult to distinguish, without an initial calibration to determine the magnitude of the response to each vapor (as in Fig. 5). Two additional experiments were therefore conducted in order to determine whether the sensor could be specific to one vapor. First, a fresh sensor was made and continuously exposed to water vapor

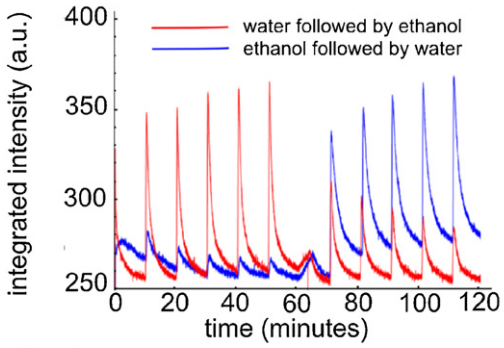

Fig. 6. Sensor response to repeated exposures to water vapor and ethanol. The blue curve shows the response to five 15-s ethanol vapor injections, followed by 5 injections of water vapor. The red line is similar, except in the reverse order. (For interpretation of the references to color in this figure legend, the reader is referred to the web version of the article.)

from a bubbler on the main line, while pumped with the laser. The sample was exposed for 50 min, which was sufficiently long for the sensor response to become saturated, with little further evolution of the fluorescence spectrum. At this point, the sensor is no longer responsive to water vapor. The water–vapor-saturated carrier gas was then diverted through a second bubbler containing ethanol. While the changes are smaller in this case, the effect of the ethanol could be clearly observed by a small rise in the integrated emission intensity every time the second bubbler was added to the gas flow (Fig. 7). In the reverse case, the sensor response was first saturated with ethanol vapor and then water was introduced in the second bubbler, for 15-s intervals. Again, a small response was clearly observed. Thus, if the magnitude of the response cannot unequivocally determine between different vapors (i.e., no pre-calibration), then a pretreatment with one vapor might make the sensor responsive to the other one.

4. Discussion

While the detailed mechanism for the sensor response will remain open to question, several lines of evidence are consistent with a set of possible surface modifications that can occur on the surface of the QDs. First, the response to ethanol

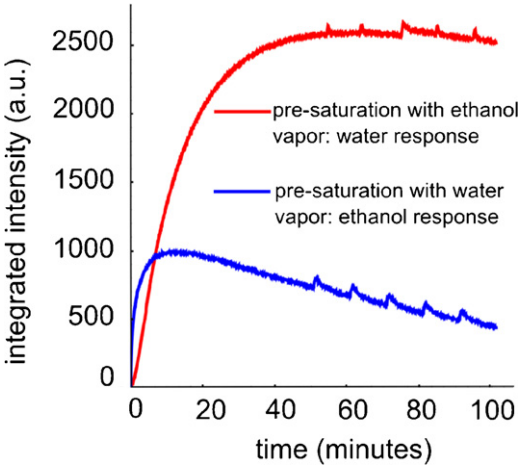

Fig. 7. The blue line shows the sensor response when the fiber was initially exposed to water vapor for 50 min. The ethanol–vapor injections are clearly observed. The red line shows the sensor response to water vapor, after being pre-saturated with ethanol. The carrier gas was O_2. (For interpretation of the references to color in this figure legend, the reader is referred to the web version of the article.)

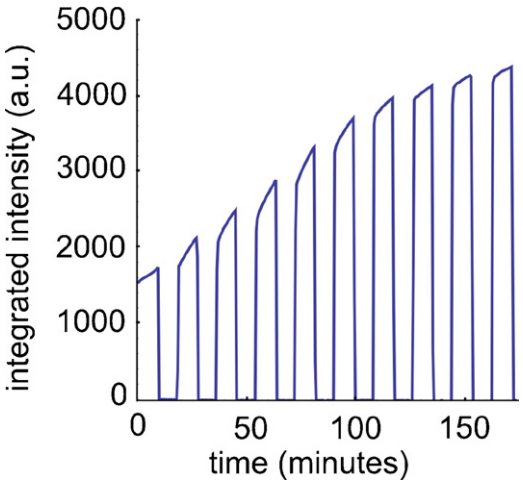

Fig. 8. Photoactivation response (integrated intensity) when the pump laser was cycled numerous times, while the sensing end of the fiber was continuously maintained in a water-saturated atmosphere. Unlike Fig. 4, the intensity of the first measurement was not subtracted in this case.

vapor is different from that to water vapor (in terms of the photoactivation rate and saturation behavior). Second, when exposed to dry O_2, the photoactivation process is at least partly reversible. Third, the response can saturate and then bleach. Fourth, a weak photoactivation can be induced when the luminescence response was first saturated in one vapor, and the QDs were then exposed to a different vapor. Fifth, the effect of the carrier gas was investigated by repeating several measurements using N_2 or Ar as the carrier gas, in place of O_2. For these atmospheres, little to no detectable photoactivation was found. Thus, O_2 in the carrier is necessary for the photoactivation process to occur at a useful rate.

The processes (photoactivation or "de-activation") do not occur without blue-light irradiation. Allowing the sensor end of the fiber coupler to "sit" in any of the investigated vapors resulted in no effect – in other words, one can partially photoactivate the QDs, turn the pump laser off while the sensor remains exposed to the analyte for 30–60 min, and when the laser is turned back on there are few changes in the fluorescence spectrum or intensity. This is illustrated in Fig. 8, in which the "active" end of the sensor was allowed to remain in a water–vapor saturated atmosphere, and the laser was turned on periodically. The overall evolution of the luminescence intensity looks mainly similar to that in Fig. 4, only interrupted by the periodic laser-off intervals.

While these present experiments cannot unambiguously determine the potentially numerous surface effects responsible for the sensor response, the fact that the response appears different for the two vapors investigated is encouraging from the point of view of making a sensor that could be specific to the desired analytes. Thus, we compare now the sensor response reported here with a selected number of alternative fiber sensors for ethanol vapor. The main points for a brief qualitative comparison are the detection limits, repeatability, response time, and cost.

In one particularly elegant example, a ring resonator was constructed for ethanol detection using evanescent coupling from a tunable laser source to measure the cavity resonances [17]. Ethanol was absorbed into the sol-gel layer of the resonator, causing the mode to shift. Detection of 31 ppm ethanol was clearly demonstrated, and sub-ppm levels could probably be probed with a sufficiently high-resolution scanning laser system. However, the maximum detection limit was close to 200 ppm, limited by the free spectral range of the resonator. In another example, ZnO nanoparticles absorbed ethanol in the vicinity of a silicon ring resonator [16], with a lower detection limit of 100 ppm.

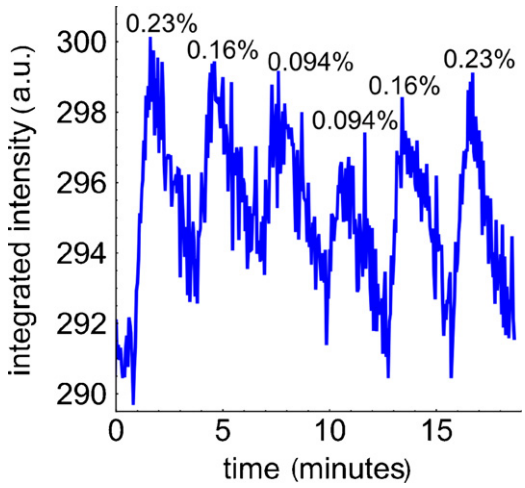

Fig. 9. Sensor response to various ethanol concentrations given as a mole percent above each peak.

In order to investigate the detection limit (DL), we made a solution of 5 vol.% ethanol dissolved in tetrahydrofuran (THF). Dry THF was found to produce no observable photoactivation, and is a solute for ethanol. The saturated ethanol concentration in the vapor is 7.3 mol.% for this mixture. This was further diluted by mixing with the oxygen carrier gas in the bubbler and combining it with a dry O_2 flow. In Fig. 9, we observe the sensor response for five 15-s exposures to vapors ranging in concentration from 0.23 to 0.094 mol.% ethanol. The sensor response was observed and was repeatable. Assuming a 3 dB signal-to-noise detection limit, from Fig. 9 we can estimate conservatively that the DL is ~380 ppm for 15-s exposure times. For longer exposures, the detection limit should decrease accordingly. In Fig. 4, we see that the 1-h response is orders of magnitude larger than it is after 15 s. This suggests that, given sufficient time, the detection limit could be reasonably low. Alternatively, the photoactivation rate can be increased by using a higher laser power. In recent work, we have found that a power as high as a few mW can be obtained in the sensor arm by using better coupling setups, although the effect of such high pump power was not investigated here.

This leads to the second point: the speed of analysis. For saturated vapors, the Si-QDs respond almost immediately, with the main delay being the ~15 s required for the vapor to reach the testing chamber. Commercial ethanol detector technologies (e.g., "breathalyzers") take a minute or less to provide a reading, with alternative sensor technologies capable of a similar range [16,17,20,28]. In the present case, as discussed above there will be a tradeoff between analysis time and detection limit. However, the photoactivation rate depends on the optical intensity on the sample [26], so better coupling of the light source to the optical fiber could simultaneously increase the speed and lower the detection limit.

We can finally evaluate, briefly, the cost and re-usability of a Si-QD-based vapor sensor. The main experimental costs are the blue light source and a means to measure the luminescence intensity. This is common to many commercial devices that require a light source and a way to measure a solution color change. In contrast, optical ring resonators require a tunable laser, which places a large premium on the cost [29]. The QD-based fiber sensor investigated here can be cycled at least 30 times by periodically breathing into the testing chamber, without a significant degradation in the response. The overall cost of a device based on Si-QDs therefore appears competitive with most proposed vapor sensing technologies.

Nevertheless, several outstanding issues must yet be addressed for this type of sensor, before any practical application can be realized. One of the most important is specificity. The Si-QD fiber sensor responds both to water vapor and to ethanol, which could make it difficult to use in "real-world" applications requiring the specific detection of alcohols. The response was different for the two cases however (Figs. 5 and 6), and can be made at least somewhat specific by pre-saturating it in the presence of the other vapor (Fig. 7). Still, in cases where the ratios of the two vapors are unknown, specificity will, at this stage, be a significant problem.

The second issue is quantification. While clear trends are observed (e.g., see Fig. 5b), true quantification of the vapor concentration in the atmosphere is currently hampered by several underlying factors. First, there is a gradual drift in the luminescence over time, since the intensity generally did not completely revert to its lowest value after each exposure. This implies that quantification would change over time. Secondly, for the lowest vapor concentrations investigated (Fig. 9), the variability in the integrated intensity under each peak is too large to clearly quantify the ethanol concentration. Thus, accurate quantification and clearly unambiguous analyte specificity are not possible with this structure, at the current time.

These issues may be related, at least in part, to sample-to-sample non-uniformity and aging. The number and concentration of QDs deposited onto the fiber surface is, at present, a significant problem that could make specificity and quantification much more difficult. This will affect not only the overall luminescence intensity, but also the overall photoactivation behavior, since large clumps like those shown in Fig. 2 contain many buried QDs that may not be well exposed to the atmosphere. This problem can lead to considerable variation between different samples or batches, and we found that it takes both experimental care and some luck with a single batch to get results that were reproducible over timescales a few days or weeks. This leads to the final issue: we observed an aging effect, in which the photoactivation properties of QDs suspended in toluene and stored in air gradually decayed over a similar period, probably as a result of gradual oxidation.

5. Conclusion

In this work, an optical fiber sensor with Si-QDs at the end facet was found to show a response to water and ethanol, a fast and reversible response time, and detection limits that could approach the range characteristic of standard ethanol sensors. The response is based on the QD fluorescence intensity which increases when the QDs are exposed under blue light irradiation to alcohol and water vapor. Reversibility is achieved by subsequent exposure to dry O_2. The magnitude of the fluorescence intensity change was found to depend on the vapor type and concentration: in 15-s exposures it was greatest for water vapor, intermediate for a water–ethanol mixture, and smallest for ethanol. The fluorescence sensor could be cycled more than 30 times without significant degradation of the performance. The work also showed the limitations of the proposed device structure, in which the two most significant were deemed to be selectivity and quantification, probably due mainly to physical clumping or agglomeration of the QDs on the fiber surface. The latter issue can lead to sample-to-sample variations in the response characteristics.

Acknowledgements

We thank the National Science and Engineering Research Council, Alberta Innovates Technology Futures and China Scholarship Council for funding this research. Thanks to Shalon McFarlane for SEM images, and Zhenyu Yang for assistance with sample etching.

References

[1] G. Gagliardi, M. Salza, S. Avino, P. Ferraro, P. De Natale, Probing the ultimate limit of fiber-optic strain sensing, Science 19 (2010) 1081–1084.
[2] M. McSherry, Review of luminescent based fibre optic temperature sensors, Sensor Review 25 (2005) 56–62.
[3] V.I. Ruiz-Pérez, M.A. Basurto-Pensado, P. LiKamWa, J.J. Sánchez-Mondragón, D.A. May-Arrioja, Fiber optic pressure sensor using multimode interference, Journal of Physics: Conference Series 274 (2011) 1–7.
[4] W.-G. Lee, D.-H. Kim, C.-G. Kim, Transmissive grating-reflective mirror-based fiber optic accelerometer for stable signal acquisition in industrial applications, Optical Engineering 51 (2012) 1–8.
[5] B. Schmauß, M. März, J. Ernst, A fiber-optic sensor for microwave field measurements, Review of Scientific Instruments 66 (1995) 4031–4033.
[6] P. Bianucci, J.R. Rodriguez, F. Lenz, C.M. Clement, J.G.C. Veinot, A. Meldrum, Silicon nanocrystal luminescence coupled to whispering gallery modes in optical fibers, Journal of Applied Physics 105 (2009) 1–5.
[7] B.R. Soller, S.O. Heard, N.A. Cingo, C. Hsi, J. Favreau, T. Khan, R.R. Ross, J.C. Puyana, Application of fiberoptic sensors for the study of hepatic dysoxia in swine hemorrhagic shock, Critical Care Medicine 29 (2001) 1438–1444.
[8] B. Lee, Review of the present status of optical fiber sensors, Optical Fiber Technology 9 (2003) 57–79.
[9] F. Baldini, A. Giannetti, A.A. Mencaglia, C. Trono, Fiber optic sensors for biomedical applications, Current Analytical Chemistry 4 (2008) 378–390.
[10] C. Elosua, I. Matias, C. Bariain, F.J. Arregui, Volatile organic compound optical fiber sensors: a review, Sensors 6 (2006) 1440–1465.
[11] M. El-Sherif, L. Bansal, J. Yuan, Fiber optic sensors for detection of toxic and biological threats, Sensors 7 (2007) 3100–3118.
[12] Y.Z. Liao, V. Strong, Y. Wang, X.G. Li, X. Wang, R.B. Kaner, Oligotriphenylene nanofiber sensors for detection of nitro-based explosives, Advanced Functional Materials 22 (2012) 726–735.
[13] H. Steiner, M. Jakusch, M. Kraft, M. Karlowatz, T. Baumann, R. Niessner, W. Konz, A. Brandenburg, K. Michel, C. Boussard-Plédel, B. Bureau, J. Lucas, Y. Reichlin, A. Katzir, N. Fleischmann, K. Staubmann, R. Allabashi, J.M. Bayona, B. Mizaikoff, In situ sensing of volatile organic compounds in groundwater: first field tests of a mid-infrared fiber-optic sensing system, Applied Spectroscopy 57 (2003) 607–613.
[14] M. Morisawa, S. Muto, Plastic optical fiber sensing of alcohol concentration in liquors, Journal of Sensors 2012 (2012) 1–5.
[15] G. Possetti, M. Muller, J.L. Fabris, Refractometric optical fiber sensor for measurement of ethanol concentration in ethanol-gasoline blend, in: Microwave and Optoelectronics Conference (IMOC), SBMO/IEEE MTT-S International, 2009, pp. 616–620.
[16] N.A. Yebo, P. Lommens, Z. Hens, R. Baets, An integrated optic ethanol vapor sensor based on a silicon-on-insulator microring resonator coated with a porous ZnO film, Optics Express 18 (2010) 11859–11866.
[17] F. Pang, X. Hana, F. Chua, J. Genga, H. Cai, R. Qua, Z. Fang, Sensitivity to alcohols of a planar waveguide ring resonator fabricated by a sol–gel method, Sensors and Actuators B 120 (2007) 610–614.
[18] M. Konstantaki, A. Klini, D. Anglos, S. Pissadakis, An ethanol vapor detection probe based on a ZnO nanorod coated optical fiber long period, Optics Express 20 (2012) 8472–8484.
[19] B. Renganathan, D. Sastikumar, G. Gobi, N.R. Yogamalar, A.C. Bose, Nanocrystalline ZnO coated fiber optic sensor for ammonia gas detection, Optics & Laser Technology 43 (2011) 1398–1404.
[20] W. Ma, H. Yang, W. Wang, P. Gao, J. Yao, Ethanol vapor sensing properties of triangular silver nanostructures based on localized surface plasmon resonance, Sensors 11 (2011) 8643–8653.
[21] E.J. Anglin, L. Cheng, W.R. Freeman, M.J. Sailor, Porous silicon in drug delivery devices and materials, Advanced Drug Delivery Reviews 60 (2008) 1266–1277.
[22] M.J. Sailor, E.C. Wu, Photoluminescence-based sensing with porous silicon films, microparticles, and nanoparticles, Advanced Functional Materials 19 (2009) 3195–3208.
[23] G. García Salgado, T. Díaz Becerril, H. Juárez Santiesteban, E. Rosendo Andrés, Porous silicon organic vapor sensor, Optical Materials 29 (2006) 51–55.
[24] J. Dian, T. Holec, I. Jelínek, J. Jindřich, J. Valenta, I. Pelant, Time evolution of photoluminescence response from porous silicon in hydrocarbon gas sensing, Physica Status Solidi A 185 (2000) 485–488.
[25] B.H. King, A.M. Ruminski, J.L. Snyder, M.J. Sailor, Optical-fiber-mounted porous silicon photonic crsytals for sensing organic vapor breakthrough in activated carbon, Advanced Materials 19 (2007) 4530–4534.
[26] R. Lockwood, S. McFarlane, J.R. Rodriguez-Nunez, X.Y. Wang, J.G.C. Veinot, A. Meldrum, Photoactivation of silicon quantum dots, Journal of Luminescence 131 (2011) 1530–1535.
[27] C.M. Hessel, E.J. Henderson, et al., Hydrogen silsesquioxane: a molecular precursor for nanocrystalline $Si-SiO_2$ composites and freestanding hydride-surface-terminated silicon nanoparticles, Chemistry of Materials 18 (2006) 6139–6146.
[28] F. Pourfayaz, A. Khodadadi, Y. Mortazavi, S.S. Mohajerzadeh, CeO_2 doped SnO_2 sensor selective to ethanol in presence of CO, LPG and CH_4, Sensors and Actuators B (2005) 172–176.
[29] Y.D. Jeong, Y.H. Won, S.O. Choi, J.H. Yoon, Tunable single-mode Fabry–Perot laser diode using a built-in external cavity and its modulation characteristics, Optics Letters 31 (2006) 2586–2588.

Biographies

Z.H. Zhang obtained her BSc from the Normal University of Luoyang in 2002. She is currently a PhD student at the University of Electronic Science and Technology China (UESTC) and a visiting student at the University of Alberta. Her interests are in the areas of sensors, nanoscale properties of doped semiconductors, and photonics.

R. Lockwood obtained a BSc from the University of Alberta in 2008, and is now a PhD student at the same location. Upon graduation, he hopes to take his research experience into academia or industry. He is especially interested in developing tools for space science, such as silicon photomultipliers for future telescopes and optical instruments. He has several years of experience working with silicon quantum dots and photonic systems.

J. Veinot received his BSc (Honours) in chemistry at the University of Western Ontario in 1994. He subsequently did doctoral studies at York University, obtaining his PhD in 1999. In 2000, Dr. Veinot received an NSERC Post-Doctoral Fellowship for organic electronics research at Northwestern University. He is currently a Professor in the Department of Chemistry at the University of Alberta and Fellow at the National Research Council of Canada National Institute of Nanotechnology. He leads a team of graduate students, PDFs and RAs who study the synthesis functional hybrid materials with applications in photonics, catalysis, energy conversion and environmental remediation.

A. Meldrum obtained a PhD in 1997 from the University of New Mexico. He then took a two-year postdoctoral fellowship at Oak Ridge National Laboratory, and subsequently signed on as an assistant professor at the University of Alberta. Now a full professor, his research interests are in silicon photonics, quantum dots, and sensing technologies.